Available online at www.sciencedirect.com
SCIENCE DIRECT
Bioorganic & Medicinal Chemistry 14 (2006) 1653–1659
Bioorganic & Medicinal Chemistry

Evaluation of aldose reductase inhibition and docking studies of some secondary metabolites, isolated from *Origanum vulgare* L. ssp. *hirtum*

Catherine Koukoulitsa,[a,*] Chariklia Zika,[b] George D. Geromichalos,[c] Vassilis J. Demopoulos[b] and Helen Skaltsa[a]

[a]*Department of Pharmacognosy and Chemistry of Natural Products, School of Pharmacy, University of Athens, Panepistimiopolis, Zografou, 15771, Athens, Greece*
[b]*Department of Pharmaceutical Chemistry, School of Pharmacy, University of Thessaloniki, 54124 Thessaloniki, Greece*
[c]*Symeonidio Research Center, Theagenio Cancer Hospital, Thessaloniki, Greece*

Received 10 August 2005; revised 3 October 2005; accepted 6 October 2005
Available online 24 October 2005

Abstract—Five polar constituents of *Origanum vulgare* L. ssp. *hirtum* were investigated for their ability to inhibit aldose reductase (ALR2), the first enzyme of the polyol pathway implicated in the secondary complications of diabetes. The most active compound was found to be lithospermic acid B. Caffeic acid was inactive as it showed no inhibitory activity against the enzyme. The order of the inhibitory activity of the remaining compounds was: rosmarinic acid >12-hydroxyjasmonic acid 12-*O*-β-glucopyranoside > *p*-menth-3-ene-1,2-diol 1-*O*-β-glucopyranoside. Docking studies have been undertaken to gain insight into the binding mode of the investigated compounds at the active site of ALR2. The predicted hydrogen bonding and hydrophobic interactions may explain the observed inhibitory activity.

1. Introduction

Aldose reductase (alditol: $NADP^+$ oxidoreductase, EC 1.1.1.21 ALR2) is a key enzyme in the polyol pathway as it catalyzes the reduction of glucose to sorbitol with concomitant conversion of NADPH to $NADP^+$. Intracellular accumulation of sorbitol has been implicated in the chronic complications of diabetes such as peripheral neuropathy, retinopathy, and cataract.[1] Therefore, the inhibition of the polyol pathway is considered to be a promising approach to control diabetes complications.

X-ray crystallographic studies on both porcine[2] and human[3,4] aldose reductases have shown that they belong to the $(\beta/\alpha)_8$ barrel class of enzymes and the coenzyme NADPH binds at the C-terminal end of the β barrel. The catalytic mechanism of aldose reductase involves binding of the substrate to the active site pocket of the enzyme/NADPH complex with subsequent hydride transfer from the nicotinamide ring to the carbonyl group. A proton is donated by Tyr48 to the carbonyl oxygen to complete the conversion of the aldehyde to alcohol.[5] The requisite structural elements of aldose reductase inhibitors (ARIs) are proposed as: (i) an aromatic ring system to form hydrophobic or π-π stacking interactions with the hydrophobic amino acid residues in the active site, and (ii) acidic ionizable groups, such as of carboxylic acids and spirohydantoins, which can anchor to the anionic binding site.[6–8]

To date, a variety of compounds have been synthesized that belong to two general classes; those containing a carboxylic acid moiety such as epalrestat, tolrestat, and zenarestat, and those having a cyclic imide represented by a spirohydantoin or related ring system such as sorbinil, fidarestat, and minalrestat.[9,10] Numerous ARIs also obtained from natural sources such as flavonoids, coumarins, stilbenes, monoterpenes, and related aromatic compounds have been reported in the literature.[11,12] According to an ethnobotanical survey in the

Abbreviations: ALR2, aldose reductase; ALR1, aldehyde reductase; OV, *Origanum vulgare*; ARIs, aldose reductase inhibitors.

Keywords: *Origanum vulgare* L. ssp. *hirtum*; Aldose reductase; Docking; GLUE.

* Corresponding author. Tel.: +3023 1093 2354; e-mail: koukoulitsa@pharm.uoa.gr

0968-0896/$ - see front matter © 2005 Elsevier Ltd. All rights reserved.
doi:10.1016/j.bmc.2005.10.013

Tafilalet region of Morocco by Eddouks et al.,[13] *Origanum vulgare* (OV) is traditionally used in control and treatment of diabetes.

In this study, we examined the inhibitory activity against rat lenses aldose reductase of the following secondary metabolites recently isolated from the polar extracts of OV growing wild in Greece: caffeic acid (**1**), rosmarinic acid (**2**), lithospermic acid B (**3**), 12-hydroxyjasmonic acid 12-*O*-β-glucopyranoside (**4**), and *p*-menth-3-ene-1,2-diol 1-*O*-β-glucopyranoside (**5**).[14] Moreover, based on previous crystallographic and molecular modeling studies, we performed docking calculations via the GLUE program (implemented in the Grid package) in order to examine the binding mode of the compounds at the active site of ALR2 and to explain the heterogenicity of their inhibitory activity.

2. Results and discussion

2.1. Determination of aldose reductase inhibition

The studied compounds **1**–**5** (Fig. 1) were evaluated for their inhibitory activity against rat lenses aldose reductase. The percent inhibition data at 10 and 100 μM are presented in Table 1. As can be seen, among the tested compounds, lithospermic acid B (**3**) exhibited the best inhibitory activity (96% at 100 μM) and rosmarinic acid (**2**) showed almost the same activity at the same concentration. The above compounds demonstrated significant activity even at 10 μM. Compound **4** showed also activity (77%) at 100 μM, which was dramatically decreased at a concentration of 10 μM (22%). The monoterpene glucoside **5** was less potent, while caffeic acid (**1**) was found to be inactive under the present experimental protocol.

Table 1. Inhibitory activity of the isolated compounds toward ALR2 and the results of the ligand docking calculations

Compound	% Inhibition (SEM)[a] at concn.		Energy binding[b] (kcal/mol)
	(10 μM)	(100 μM)	
1	—	8 ± 4.6	−7.68
2	66 ± 1.4	95 ± 0.0	−15.71
3	71 ± 0.0	96 ± 1.7	−16.08
4	22 ± 3.2	77 ± 1.4	−14.58
5	—	41 ± 0.6	−10.57

[a] $n = 3$.
[b] Calculated binding energy for the highest ranked docking solution.

2.2. Docking studies of receptor–ligand interactions

The difference in activity of our compounds toward aldose reductase shown in the experiments could be explained by docking calculations. The crystal structure of rat aldose reductase has not yet been reported. However, the amino acids associated with NADPH binding are strictly conserved between rat and human, and there is 85% amino acid identity between these two species.[15] Since the composition of the active site is quite similar, we selected for the docking studies the human aldose reductase holoenzyme complexed with IDD 594 (Fig. 2) (PDB entry 1US0), as it was determined at the highest resolution (0.66 Å) among all the available structures in the PDB-database.[16] The X-ray crystallography study revealed that the inhibitor IDD 594 induces a conformational change upon binding to ALR2, creating a specificity pocket localized between Phe122, Trp111,

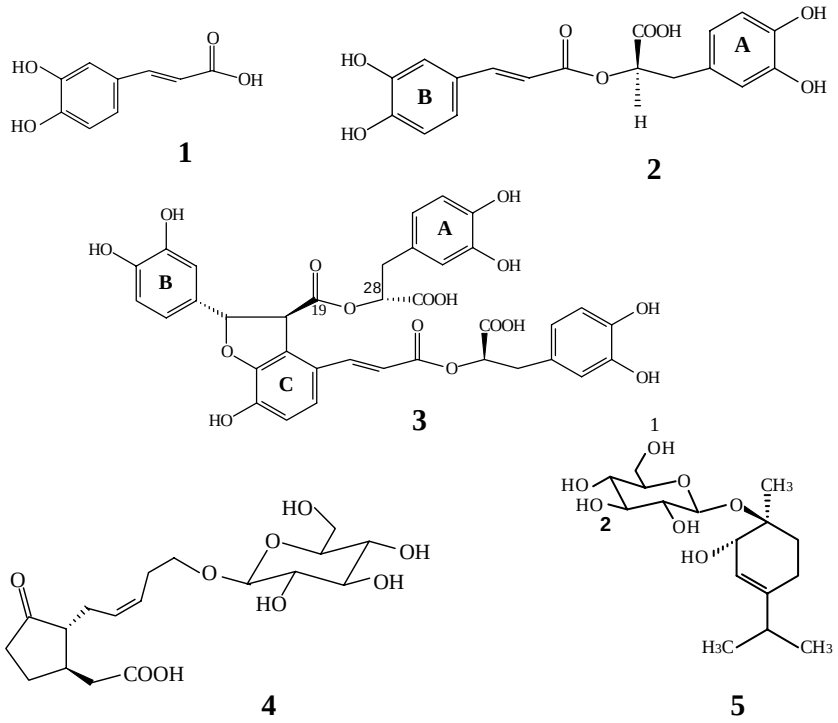

Figure 1. Structures of the investigated compounds **1**–**5**.

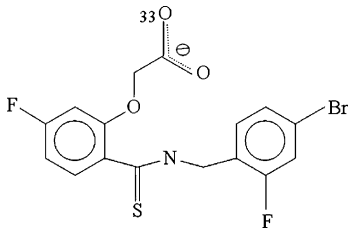

Figure 2. Structure of the inhibitor IDD 594.

Leu300, and Ala299. Compounds that bind to this specificity pocket possess much higher selectivity for ALR2 as compared with aldehyde reductase (ALR1),[17] a closely related enzyme that coexists with ALR2 in most tissues and its inhibition might cause undesired side effects.[9] The interactions of IDD 594 in the catalytic site of ALR2 are mostly polar. The carboxylate group is firmly anchored in the active site with hydrogen bonds to His110, Tyr48, and Trp111 and with a strong electrostatic interaction with $NADP^+$. From the crystallographic study it is shown that His110 is singly protonated at Nε2, as the C–Nε2 bond length is significantly longer than the C–ND1 and for this reason His110 is the proton donor in the H-bond with the carboxylate oxygen 33 of the inhibitor IDD 594. Tyr48 is also a proton donor in another H-bond to this oxygen. The coenzyme is in a charged state of $NADP^+$, as shown by the planarity of the ring and the presence of the hydrogen atom of C-4 in the plane of nicotinamide.

The docking simulations in the active site of ALR2 were performed by the docking GLUE program, which has been shown to successfully reproduce experimentally observed binding modes in terms of rmsd (root-mean squared deviation).[18,19] The crystallographic structure of IDD 594 docked into ALR2 and GLUE provided an excellent result as was observed by a low value of r.m.s.d (best docked solution of 0.34 Å) between the experimental and the calculated docked structure (Fig. 3). The ability to accurately predict the binding conformation of IDD 594 of ALR2 gave confidence that GLUE would exhibit a similar accuracy with the investigated molecules utilized in the study.

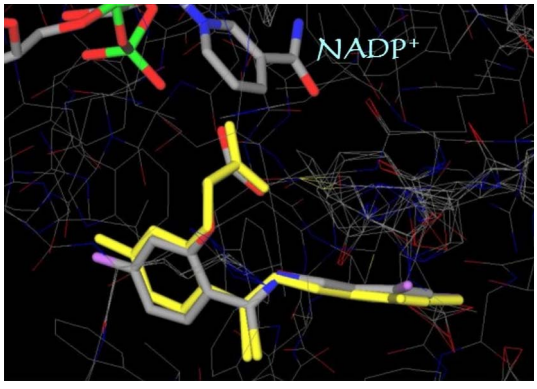

Figure 3. Conformational comparison between X-ray structure of IDD 594 (colored by atom type) and predicted (colored yellow) by GLUE.

The best possible binding modes of the five inhibitors at the aldose reductase active site are displayed in Figure 4 and their corresponding binding energies are shown in Table 1. As illustrated, the ligands were placed in the same location as IDD 594 in the crystal structure. However, in contrast to IDD 594, it is observed that there is no binding at the specificity pocket suggesting a non-selective inhibition. Given the lower pK_a of compounds **1**–**4** (pK_a values: 2.06–4.61), the carboxylic moiety is probably bound by ALR2 in its anionic form with the negative charge shared between the carboxylic oxygens. According to the observations of crystal structures of ALR2 complexed with carboxylic acid inhibitors, compounds **1**–**4** are bound to ALR2 with the carboxylate group entering the anionic binding site.[2]

In particular, rosmarinic acid (**2**) is oriented so that O1 acceptor develops hydrogen bonds with His110 (O1···H–Nε2 2.3 Å), and Trp111 (O1···H–Nε1 2.5 Å); hydrogen bonds are also formed by O2 with Tyr48 (O2···H–O 2.0 Å), His110 (O2···H–Nε2 1.8 Å) and Trp111 (O2···H–Nε1 3.4 Å). The carboxylate moiety is also anchored to the anionic binding site through electrostatic interactions with the positively charged nicotinamide ring of $NADP^+$. Phenyl ring A is positioned at the opening of the specificity pocket stabilized by aromatic interactions with Trp79, Trp111, and Trp219, and van der Waals interactions with residues Phe122, Ala299, and Leu300. Hydrophobic interactions are also observed at phenyl ring B with residues Trp79 and Phe122.

In lithospermic acid B (**3**), the carboxylate group of the position C-28 is anchored in the anionic binding site forming hydrogen bonds with Tyr48, His110, and Trp111. Interestingly, polar interactions are observed within the hydrophobic pocket between the oxygen at C-19 with Nε1 of Trp20. The higher predicted binding energy of lithospermic acid B compared to that of rosmarinic acid reflects also its potential in forming numerous hydrophobic interactions in the active site of ALR2. Indeed, phenyl ring A located at the opening of the specificity pocket makes contacts with Trp20, Trp79, Trp111, and Ala299, phenyl ring B with Phe122, Trp219, and Leu300, and phenyl ring C with Trp20 and Phe121. Since the binding pocket of ALR2 is rather hydrophobic, the predicted binding mode and the inhibitory activity of lithospermic acid B may be reasoned by its comparatively higher lipophilicity, as was documented by its calculated log *P* value of the anion form of the docked conformer: 3.27 (caffeic acid: 0.51, rosmarinic acid: 2.12, 12-hydroxyjasmonic acid 12-*O*-β-glucopyranoside: −2.95). In Figure 5 is illustrated the hydrophobic region in the active pocket with the docked conformation of lithospermic acid B.

Compound **4** forms hydrogen bonds with Tyr48, His110 and Trp111 through the carboxylate moiety and electrostatic interactions with $NADP^+$. The cyclopentanone group is inserted in the hydrophobic pocket making contacts with residues Trp20, Trp79, Phe122, Pro218, Trp219 and Leu300. The lower predicted binding affinity of compound **4** compared to those of compounds

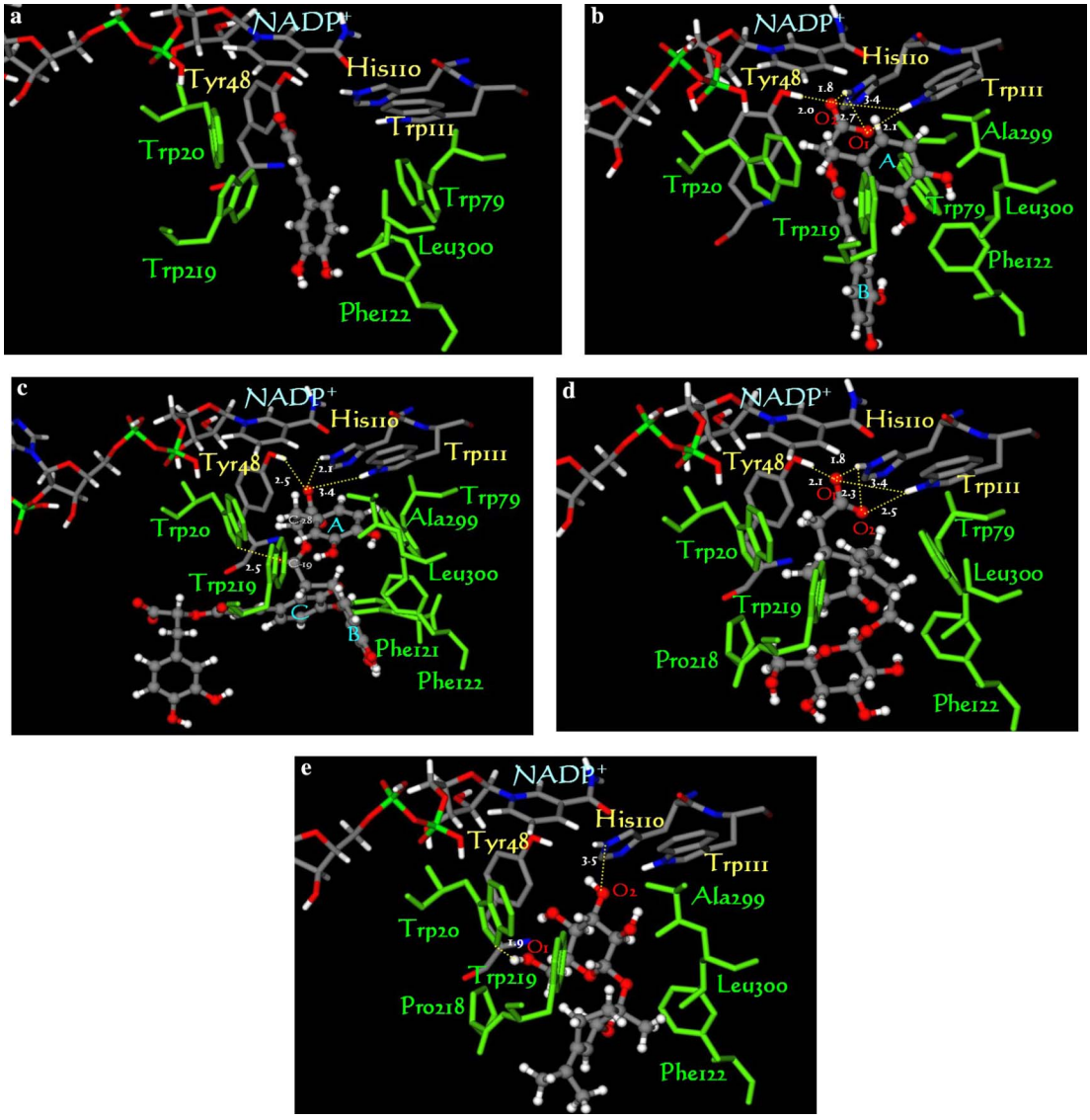

Figure 4. Docked orientations of (a) caffeic acid (**1**); (b) rosmarinic acid (**2**); (c) lithospermic acid B (**3**); (d) 12-hydroxyjasmonic acid 12-*O*-β-glucopyranoside (**4**) and (e) *p*-menth-3-ene-1,2-diol 1-*O*-β-glucopyranoside (**5**) with additional depiction of selected aminoacid residues of ALR2 active site. Hydrogen bonds and polar interactions are shown as dotted lines.

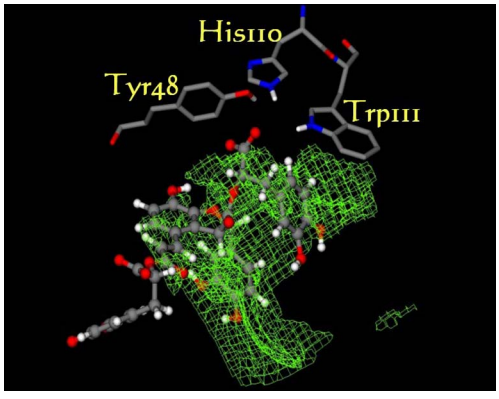

Figure 5. Visualization of the contour plot of GRID hydrophobic field calculated with DRY probe at −0.2 kcal/mol in the active site (the calculation was performed by Greater program implemented in the GRID package). The docked conformation of lithospermic acid B is displayed.

rosmarinic acid (**2**) and lithospermic acid B (**3**) could reflect its lower activity.

Although caffeic acid (**1**) entered the anionic binding site with the carboxylate moiety, it could not establish strong interactions with the key aminoacid residues and $NADP^+$. Only few contacts with the residues of the hydrophobic pocket are observed. The results from the docking calculations are consistent with the lower estimated binding energy and the observed inactivity of caffeic acid against aldose reductase (Table 1).

In compound **5**, the glucoside moiety was located in the anionic hole forming weak hydrogen bonds with the imidazolium Nε2 of His110 (3.5 Å) and the nitrogen of $NADP^+$ (3.6 Å). Further weaker electrostatic interactions between the aforementioned hydroxyl group and the positively charge $NADP^+$ were observed (5.9 Å). The stabilization of the compound in the pocket was

attributed to the hydrogen bond formed by a hydroxyl group with the Nε1 of Trp20 (1.9 Å) and the hydrophobic contacts of the terpenoid moiety with the residues Phe122, Pro218, Trp219, Ala299, and Leu300. In accordance with these results, compound **5** is consistent with the observed weaker activity among the investigated compounds.

Molecular modeling studies can further explain the interaction between the docked conformations of the investigated compounds with aminoacids Tyr48 and His110. In Figure 6, there are depicted the maps of electrostatic potential along with the HOMO of compounds **2**–**5**. As illustrated in this figure, it is interesting to note that in lithospermic acid B (**3**) that possess two carboxylic groups, the HOMO and the most negative electrostatic potential (value: −187.306 kcal/mol) is located on the carboxylic oxygen that interacts with His110 and Tyr48. On the contrary, the electrostatic potential value of the non-interacting carboxylic oxygen is −91.260 kcal/mol. The same localization of the HOMO and the most negative electrostatic potential is also observed for the remaining compounds. The most negative calculated electrostatic potential values were: −208.377 kcal/mol (O1) and −193.045 kcal/mol (O2) for rosmarinic acid (**2**), −194.069 kcal/mol (O1) and −190.495 kcal/mol (O2) for 12-hydroxyjasmonic acid 12-*O*-β-glucopyranoside (**4**), and −44.659 kcal/mol (O1) and −47.941 kcal/mol (O2) for *p*-menth-3-ene-1,2-diol 1-*O*-β-glucopyranoside (**5**). From the above values, it is interesting to note that in compound **5** the negative electrostatic potential value of O2 is lower than those of the carboxylic oxygens of the examined compounds. Based on this consideration its weaker electrostatic interaction between the oxygen of the hydroxyl group on O2 and the nitrogen Nε2 of His110 could be explained. The smaller hydrogen bond distances between the interactive carboxylic oxygen of compounds and the hydrogen of Nε2 of His110 compared to the corresponding hydrogen bond with the hydroxyl hydrogen of Tyr48 can be reasoned by the most positive electrostatic potential of His110 hydrogen (39.798 kcal/mol vs 35.053 kcal/mol of Tyr48). The hydrogen charge of Tyr48 contributing to the hydrogen bond is more positive (0.375) compared to His110 hydrogen (0.141). This may be suggestive of a more hydrogen bond donor character.

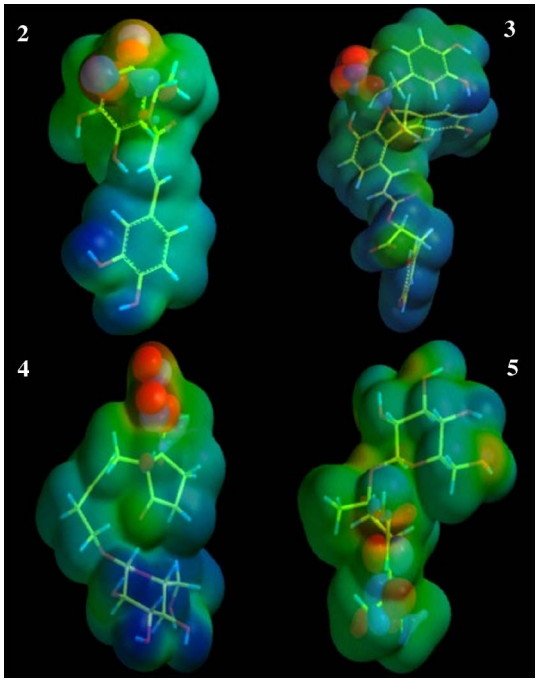

Figure 6. Illustration of the electrostatic potential map (transparent) along with the HOMO orbital (solid) of compounds **2**–**5**.

3. Conclusion

The inhibitory activity against rat lenses aldose reductase of compounds **1**–**5** was examined and docking studies on the active site of the enzyme were performed. Lithospermic acid B was the most active compound. Future research will focus on the investigation of the ability of the studied compounds to inhibit also lipoxygenase, since cellular and animal model studies indicated the induction of proinflammatory enzymes, such as 15-lipoxygenase, under diabetic conditions.[20]

Docking results seem to support the biological data. Despite the fact that carboxylic acids have a potent inhibitory activity in vitro, they are less potent in vivo due to their complete dissociation at physiological pH.[21] On this basis, a design of semisynthetic compounds is in progress aiming at the substitution of the carboxylic moiety by an appropriate group of higher pK_a values that, also, would establish strong interactions with the key residues of the active site of the enzyme. Docking studies on a virtual library of semisynthetic products will be useful in order to discover promising compounds.

4. Experimental

4.1. Isolation and identification of the examined compounds

The compounds were extracted from the aerial parts of *O. vulgare* L. ssp. *hirtum*. The plant was collected from Pogoni-Ioannina (Epirus, North-Western Greece) in July 2002 and authenticated by Dr. Th. Constantinidis (Institute of Systematic Botany, Agricultural University of Athens). A voucher specimen is deposited at the Herbarium of the Institute of Systematic Botany, Agricultural University of Athens (ACA), Lazari 1.

The isolation and the structure elucidation of the isolated compounds were described by the authors Koukoulitsa et al.[14]

4.2. Determination of aldose reductase inhibition in vitro

The studied compounds as well as sorbinil ($C_{11}H_9FN_2O_3$, reference) were dissolved in 0.2 M $NaHCO_3$. Lenses were quickly removed from Fischer-344 rats of both sexes following euthanasia, and enzyme preparation and assay were performed as previously

described.[22–24] All experiments were performed in triplicate. Results are shown in Table 1.

It should be noted that the aldose reductase inhibitory activity has been previously reported for the compounds: caffeic acid (**1**),[25] rosmarinic acid (**2**)[26], and lithospermic acid B (**3**).[26] However, the results were obtained using different experimental protocols than ours.

4.3. Computational methods

The considered molecules were built in 3D coordinates and their most stable (lower energy) conformations were calculated, by geometrical optimization of their structure as implemented in the Spartan '04 Molecular Modeling program suite,[27] utilizing MMFF and PM3 semi-empirical methods. The X-ray structure of human aldose reductase holoenzyme (PDB 1US0) was used in our docking calculations after deletion of the inhibitor IDD 594 from the PDB file, obtained from the Brookhaven Protein Data Bank.[28]

Docking calculations were performed with GLUE program implemented in the GRID package (www.moldiscovery.com).[29] GLUE[18] is a docking procedure aimed at detecting energetically favorable binding modes of a ligand with respect to the protein active site using the GRID force field.[30] The protein cavity is mapped using several GRID runs: a set of different probes is used to mimic all chemical groups present in the ligand and the resulting maps are encoded into compact files which store the interaction energies. Afterwards, an iterative procedure identifies all the ways in which four atoms of the ligand could bind to the target, by pairing every atom to the 'nearest' MIF used. Hydrophobic and polar atoms of the ligand for which several conformers are quickly produced are fitted over their corresponding energy maps, giving rise to sometimes millions of ligand orientations, which are temporarily stored. Then, many orientations are quickly eliminated due to redundancy and steric hindrance constraints. Redundancy occurs whenever two or more orientations are close enough to each other, that is, the rmsd calculated over their 3D structures is lower than 2.0 Å; therefore, they are grouped and one orientation represents the entire group. Conversely, steric hindrance occurs whenever part of the ligand clashes into the binding site: in this case, the clashing part is accommodated along the site if possible; otherwise, the orientation is excluded. Indeed, this refinement allows only reliable orientations to be processed in the next step: each orientation is optimized within the cavity by means of successive torsions and translations. These are driven by the ligand–target interaction energy computed by the GRID force field: each little movement is followed by an energy reassessment according to the GRID standard equation applied over the whole ligand and the active site:

$$E\mathrm{GRID} = \mathrm{ELJ} + E\mathrm{EL} + E\mathrm{HB} + E\mathrm{ENTROPY}$$

The optimized orientations represent possible binding modes of the ligand within the site. The interaction energy between the entire ligand and the protein binding site is calculated by using the GLUE equation, which provides an energy scoring function (*E*GLUE) composed by four contributions: *E*SR = steric repulsion energy, *E*ES = electrostatic energy, *E*RHB = hydrogen bonding charge reinforcement, and *E*DRY = hydrophobic energy.

$$E\mathrm{GLUE} = E\mathrm{SR} + E\mathrm{ES} + E\mathrm{RHB} + E\mathrm{DRY}$$

The final output of the docking procedure is a set of solutions ranked according to the corresponding scoring function values, each defined by the 3D coordinates of its atoms and expressed as a PDB file.

The docked structures were imported into the Spartan, and the electrostatic potential and HOMO values were determined by using PM3 (single point) semiempirical calculation.

The lipophilicity log *P* was calculated by VolSurf program[31,32] (version 4.1.3, www.moldiscovery.com).

The pK_a values for compounds **1**–**4** were calculated by Pallas program[33] (version 3.1.1.2, www.compudrug.com).

Gview molecular graphic system (implemented in the GRID package) was used in order to visualize the molecules and the results of docking.

Acknowledgments

We are grateful to Prof. Gabriele Cruciani (Laboratory for Chemometrics, School of Chemistry, University of Perugia, Italy) for providing us GRID package, VolSurf program and for helpful advices. We are also thankful to Dr. Anna Tsantili-Kakoulidou for the permission to use Pallas program.

References and notes

1. Kinoshita, J. H.; Nishimura, C. *Diabetes Metab. Rev.* **1988**, *4*, 323.
2. Urzhumtsev, A.; Tête-Favier, F.; Mitschler, A.; Barbanton, J.; Bath, P.; Urzhumtseva, L.; Biellmann, J.-F.; Podjarny, A. D.; Moras, D. *Structure* **1997**, *5*, 601.
3. Wilson, D.; Bohren, K. M.; Gabbay, K. H.; Quiocho, F. A. *Science* **1992**, *257*, 81.
4. Harrison, D. H.; Bohren, K. M.; Ringe, D.; Petsko, G. A.; Gabbay, K. H. *Biochemistry* **1994**, *33*, 2011.
5. Ehrig, T.; Bohren, K. M.; Prendergast, F. G.; Gabbay, K. H. *Biochemistry* **1994**, *33*, 7157.
6. Miyamoto, S. *Chem-Bio Informatics Journal* **2002**, *2*, 74.
7. Lee, Y. S.; Chen, Z.; Kador, P. F. *Bioorg. Med. Chem.* **1998**, *6*, 1811.
8. Sun, W. S.; Park, Y. S.; Yoo, J.; Park, K. D.; Kim, S. H.; Kim, J. H.; Park, H.-J. *J. Med. Chem.* **2003**, *46*, 5619.
9. Miyamoto, S. *Expert Opin. Ther. Patents* **2002**, *12*, 621.
10. Demopoulos, V. J.; Zaher, N.; Zika, C.; Anagnostou, C.; Mamadou, E.; Alexiou, P.; Nicolaou, I. *Drug Design Reviews-Online* **2005**, *2*, 293.
11. Kawanishi, K.; Ueda, H.; Moriyasu, M. *Curr. Med. Chem.* **2003**, *10*, 1353.

12. De la Fuente, J. A.; Manzanaro, S. *Nat. Prod. Rep.* **2003**, *20*, 243.
13. Eddouks, M.; Maghrani, M.; Lemhadri, A.; Ouahidi, M.-L.; Jouad, H. *J. Ethnopharmacol.* **2002**, *82*, 97.
14. Koukoulitsa, C.; Karioti, A.; Bergonzi, M. C.; Geromichalos, G. D.; Pescitelli, G.; Di Bari, L.; Skaltsa, H. Manuscript in preparation.
15. El-Kabbani, O.; Ramsland, P.; Darmanin, C.; Chung, R. P.-T.; Podjarny, A. *Proteins* **2003**, *50*, 230.
16. Howard, E. I.; Sanishvili, R.; Cachau, R. E.; Mitschler, A.; Chevrier, B.; Barth, P.; Lamour, V.; Van Zandt, M.; Sibley, E.; Bon, C.; Moras, D.; Schneider, T. R.; Joachimiak, A.; Podjarny, A. *Proteins* **2004**, *55*, 792.
17. Urzhumtsev, A.; Tête-Favier, F.; Mitschler, A.; Barbanton, J.; Bath, P.; Urzhumtseva, L.; Biellmann, J.-F.; Podjarny, A. D.; Moras, D. *Structure* **1997**, *5*, 601.
18. Carosati, E.; Sciabola, S.; Cruciani, G. *J. Med. Chem.* **2004**, *47*, 5114.
19. Sciabola, S.; Carosati, E.; Baroni, M.; Mannhold, R. *J. Med. Chem.* **2005**, *48*, 3756.
20. Natarjan, R.; Nadler, J. L. *Arterioscler. Thromb. Vasc. Biol.* **2004**, *24*, 1542.
21. Mylari, B. L.; Armento, S. J.; Beebe, D. A.; Conn, E. L.; Coutcher, J. B.; Dina, M. S.; O'Gorman, M. T.; Linhares, M. C.; Martin, W. H.; Oates, P. J.; Tess, D. A.; Withbroe, G. J.; Zembrowski, W. J. *J. Med. Chem.* **2003**, *46*, 2283.
22. Nikolaou, I.; Zika, C.; Demopoulos, V. J. *J. Med. Chem.* **2004**, *47*, 2706.
23. Nikolaou, I.; Demopoulos, V. J. *J. Med. Chem.* **2003**, *46*, 417.
24. Zaher, N.; Nikolaou, I.; Demopoulos, V. J. *J. Enzyme Inhib. Med. Chem.* **2002**, *17*, 131.
25. Terashima, S.; Shimizu, M.; Horie, S.; Morita, N. *Chem. Pharm. Bull.* **1991**, *39*, 3346.
26. Kasimu, R.; Tanaka, K.; Tezuka, Y.; Gong, Z. N.; Li, J. X.; Basnet, P.; Namba, T.; Kadota, S. *Chem. Pharm. Bull.* **1998**, *46*, 500.
27. Spartan '04 Windows, Wavefunction, Irving, CA.
28. RCSB Protein Data Bank, operated by the Research Collaboratory for Structural Bioinformatics.
29. GRID version 22, Molecular Discovery Ltd., 4. Chandos Street, W1A 3BQ, London, UK.
30. Goodford, P. J. *J. Med. Chem.* **1985**, *28*, 849.
31. Cruciani, G.; Crivori, P.; Carrupt, P.-A.; Testa, B. J. *J. Mol. Struct.: THEOCHEM* **2000**, *503*, 17.
32. Cruciani, G.; Pastor, M.; Guba, W. *Eur. J. Pharm. Sci.* **2000**, *11*(Suppl. 2), S29.
33. Pallas version 3.1.1.2, CompuDrug International, 115 Morgan Drive, Sedona, AZ 86351, USA.